Lipid rafts mediate biosynthetic transport to the T lymphocyte uropod subdomain and are necessary for uropod integrity and function

Jaime Millán, María C. Montoya, David Sancho, Francisco Sánchez-Madrid, and Miguel A. Alonso

Polarized migrating T cells possess 2 poles, the uropod protrusion at the rear and the leading edge at the front, with specific protein composition and function. The influenza virus hemagglutinin (HA) is a prototypical molecule that uses lipid rafts for biosynthetic transport to the apical surface in polarized epithelial Madin-Darby canine kidney (MDCK) cells. In this study, HA was used as a tool to investigate the role of lipid rafts in vectorial protein traffic in polarized T lymphocytes. Results show that newly synthesized HA becomes selectively targeted to the uropod subdomain in polarized T lymphoblasts. HA incorporates into rafts soon after biosynthesis, suggesting that delivery of HA to the uropod occurs through a pathway of transport reminiscent of that used for its specific targeting to the apical surface. HA and the adhesion molecules, intercellular adhesion molecule 3 (ICAM-3), CD44, and CD43, 3 endogenous uropod markers, were detected in surface rafts of T lymphoblasts. Cholesterol, a major component of lipid rafts, was predominantly located in the uropod. Disruption of lipid raft integrity by cholesterol sequestration produced unclustering of ICAM-3 and the loss of uropodia and severely impaired processes that require a polarized phenotype such as intercellular aggregation and cell migration. Collectively, these results indicate that lipid rafts constitute a route for selective targeting of proteins to the uropod and that the rafts are essential for the generation, maintenance, and functionality of T-cell anteroposterior polarity. (Blood. 2002;99:978-984)

Introduction

Cell polarization involves segregation of specific molecules into distinct surface subdomains and the subsequent stabilization of those subdomains by cytoskeletal forces. Polarized distribution of molecules is often accompanied by a morphologic spatial asymmetry in the cell surface that is evidenced by the existence of distinct surface specializations as it occurs with the apical and basolateral surfaces in polarized epithelia and the axonal and dendritic processes in neurons.[1] In other cell types, the polarized morphology is only evident when the cells carry out certain functions, such as migration in fibroblasts or cell-cell interactions by T lymphocytes.[2-4] In general, migration involves the spatial segregation along the axis of the cell of a leading edge, which is enriched in receptors involved in recognition of chemoattractants and substrate-adhesion molecules, and a trailing edge where the bulk of the endocytic trafficking is concentrated.[5,6] Unlike other migrating cell types, the poles of a migrating T cell display specific features related to the specialized function of these cells in the immune response.[7] Thus, in addition to its role in adhesion to the substrate, the leading edge in T lymphocytes constitutes a zone of high sensitivity to antigen and to chemotactic cytokines,[8,9] whereas the trailing end forms a characteristic membrane protrusion, termed the uropod.[10] The uropod selectively concentrates molecules involved in intercellular adhesion, such as intercellular adhesion molecule (ICAM) 1 to 3, P-selectin glycoprotein ligand (PSGL-1) CD43, and CD44, and appears depleted of integrins and receptors characteristic of the leading edge.[11] The acquisition of the uropod–leading edge polarized phenotype can be induced in T cells by exposure to chemokines and proinflammatory mediators[11-13] or by ligation with antibodies to certain surface molecules.[10,14] Recently, novel functions have been assigned to the uropod, including presentation of growth factors by syndecan[15] or induction of programmed cell death through redistributed Fas molecules.[16] The specific delivery of molecules to the different plasma membrane subdomains through specialized pathways of transport plays a major role in the generation and maintenance of apical-basolateral or axonal-somatodendritic asymmetry in epithelia and neurons, respectively.[1,17,18] In the case of polarized T lymphocytes, however, the existence of similar pathways remains largely unexplored.

The existence and role of lipid microdomains or rafts are yielding new insights into the dynamic processes occurring in cellular membranes.[19] Unlike the bulk of membranes, which are enriched in phospholipids and packed in a disordered state, rafts have a high glycosphingolipid and cholesterol content and appear to be packed in a liquid-ordered structure.[20] These features allow the isolation of lipid rafts as a detergent-insoluble membrane fraction.[21] Recruitment of specific proteins into rafts was initially proposed to explain the segregation and transport of apical proteins during biosynthetic transport in polarized epithelial cells,[22] and more recently it has been put forward as a general mechanism for protein recruitment in a variety of processes including membrane

From the Centro de Biología Molecular "Severo Ochoa," Universidad Autónoma de Madrid, Consejo Superior de Investigaciones Científicas and Servicio de Inmunología, Hospital de la Princesa, Universidad Autónoma de Madrid, Spain.

Submitted May 24, 2001; accepted September 30, 2001.

Supported by grants from the Ministerio de Ciencia y Tecnología (PM99-0092), Fondo de Investigación Sanitaria (01/0085-01), and Comunidad de Madrid (08.3/0020/1998) to M.A.A. and from the Ministerio de Ciencia y Tecnología (SAF99-0034-C01, FEDER FD97-068-C02-02) and European Community (QRLT-1999-01036) (F.S.-M.). J.M. and M.C.M. are supported by postdoctoral fellowships from the Comunidad de Madrid. D.S. is supported by a "Severo Ochoa" fellowship from the Fundación Ferrer (Barcelona, Spain).

Reprints: Miguel A. Alonso, Centro de Biología Molecular "Severo Ochoa," Universidad Autónoma de Madrid, Cantoblanco 28049-Madrid, Spain; e-mail: maalonso@cbm.uam.es.

The publication costs of this article were defrayed in part by page charge payment. Therefore, and solely to indicate this fact, this article is hereby marked "advertisement" in accordance with 18 U.S.C. section 1734.

trafficking and signaling.[19] The existence in polarized epithelial Madin-Darby canine kidney (MDCK) cells of a lipid raft–mediated pathway for apical transport is supported by the observations that the influenza virus hemagglutinin (HA), a paradigm of apical protein, becomes incorporated into internal lipid rafts soon after biosynthesis,[23] and its delivery to the apical membrane is sensitive to lipid raft disruption.[24] The integral protein machinery involved in this raft-mediated pathway in epithelial cells has just begun to be deciphered.[25-28]

The identification of functional rafts in T cells[29-31] and the fact that polarized T cells possess 2 poles with specific protein composition and function[3] led us to investigate whether lipid rafts play a role in vectorial transport of newly synthesized molecules to specific T-cell membrane subdomains and to examine the requirement for rafts in T-cell functions carried out by polarized lymphocytes. Our results indicate that lipid rafts mediate a biosynthetic pathway for protein delivery to the uropod pole and that lipid rafts are essential for the generation and maintenance of the morphologic, biochemical, and functional polarity of T lymphocytes.

Materials and methods

Reagents and antibodies

The monoclonal antibodies (mAbs) TP1/24 and HP2/19 to ICAM-3, HP2/9 to CD44, and D3/9 to CD45 have been described previously.[32] The rabbit polyclonal antiserum to ICAM-3 was kindly provided by Dr D. Simmons (John Radcliffe Hospital, Oxford, United Kingdom). Anti-HA mAb and anti-CD43 mAb MEM-59 were kind gifts from Dr E. Rodriguez-Boulan (Cornell University, Ithaca, NY) and Dr V. Horejsi (Institute of Molecular Genetics, Prague, Czech Republic), respectively. Fluorescent phalloidin and antibodies to α- or γ-tubulin were from Molecular Probes (Eugene, OR) and Amersham Pharmacia Biotech (Uppsala, Sweden), respectively. Fluorescein- or Texas red–conjugated secondary anti-IgG or IgG antibodies were from Pierce (Rockford, IL). Peroxidase-conjugated secondary anti-IgG antibodies, sulfo-N-hydroxyl-succinimido-biotin (sulfo-NHS-biotin), streptavidin-coupled agarose, and peroxidase-coupled streptavidin were supplied by Pierce. The anti-58K Golgi marker mAb, Triton X-100, filipin, methyl-β-cyclodextrin (CD), and cholera toxin B subunit coupled to peroxidase were purchased from Sigma Chemical (St Louis, MO). The chemokines stromal-derived factor (SDF-1α) and RANTES were from R & D Systems (Minneapolis, MN).

Cell culture conditions and influenza virus infection

Human T lymphoblasts were prepared from peripheral blood mononuclear cells by treatment with 0.5% phytohemagglutinin (Amersham Pharmacia Biotech) for 48 hours. Cells were washed and cultured in RPMI 1640 medium containing 10% fetal calf serum (FCS) and 2 U/mL interleukin-2 (IL-2) in an atmosphere of 5% CO_2/95% air. T lymphoblasts cultured for 7 to 12 days were typically used in all the experiments. In agreement with previous reports,[11] 30% to 40% of the cells in the culture displayed a polarized morphology under these conditions. Influenza virus A WSN strain (a generous gift from Dr E. Rodriguez-Boulan) was grown and titered on MDCK cells. T lymphoblasts or Jurkat cells were incubated with influenza virus (10-15 plaque-forming units/cell) for 1 hour at 37°C to allow adsorption and entry of the virus. After that (taken as time zero of infection), the inoculum was removed and the cell cultures incubated in normal medium at 37°C for the indicated times.

Immunoprecipitation analysis

For metabolic labeling, cells were starved in culture medium lacking methionine and cysteine for 30 minutes and incubated with 100 to 500 μCi (3.7-18.5 × 10^6 Bq) of a (^{35}S)methionine/cysteine mixture (ICN, Costa Mesa, CA) for 5 minutes at 37°C. After this period, the medium was removed and replaced with standard culture medium. For immunoprecipitation of HA during biosynthetic transport, antibodies were prebound overnight at 4°C to protein G-Sepharose in 10 mM Tris-HCl, pH 8.0, 0.15 M NaCl, 1% Triton X-100. Cell extracts were incubated for 4 hours at 4°C with control antibodies bound to protein G-Sepharose, and the supernatant immunoprecipitated by incubation for 4 hours at 4°C with the appropriate antibodies bound to protein G-Sepharose. After collection, the immunoprecipitates were washed 6 times with 1 mL 10 mM Tris-HCl, pH 8.0, 0.15 M NaCl, 1% Triton X-100, and analyzed by sodium dodecyl sulfate-polyacrylamide gel electrophoresis (SDS-PAGE) under reducing conditions. To detect ^{35}S-labeling, dried gels were finally exposed to Fujifilm imaging plates (Fuji Photo Film, Tokyo, Japan). Immunoprecipitation of surface-biotinylated proteins was carried out with streptavidin-agarose using a protocol similar to that described for immunoprecipitation with antibodies bound to protein G-Sepharose. To detect surface labeling, immunoprecipitates were subjected to immunoblot analysis with streptavidin conjugated to peroxidase and developed using the enhanced chemiluminescence ECL Western blotting kit (Amersham Pharmacia Biotech).

Detergent extraction procedures

T cells (1.0 × 10^8 cells) were washed and lysed for 30 minutes in 25 mM Tris-HCl, pH 7.4, 150 mM NaCl, 0.2% Triton X-100 at 4°C. Lipid rafts were isolated by standard procedures.[21] Briefly, the lysate was homogenized by passing the sample through a 22-gauge needle, brought to 40% sucrose (wt/wt) in a final volume of 4 mL, and placed at the bottom of an 8-mL 5% to 30% linear sucrose density gradient. Gradients were centrifuged to equilibrium for 18 hours at 39 000 rpm at 4°C in a Beckman SW41 rotor. Fractions of 1 mL were harvested from the bottom of the tube. The soluble (fractions 1-4) and the insoluble (fractions 7-9) fractions were separately pooled. To follow the incorporation of HA into lipid rafts after biosynthesis, equivalent aliquots from the soluble (S) fraction and the insoluble (I) floating membrane fraction were autoradiographed. Octyl-glucoside is a gentle detergent that solubilizes lipid rafts but does not disrupt cytoskeletal protein-protein interactions.[21] For the analysis of surface rafts associated with the cytoskeleton, the pellet fraction from surface biotinylated cells was solubilized with 1% Triton X-100 plus 60 mM octyl-glucoside at 37°C, and the solubilized raft components (fraction P) were separated from nuclei and the protein cytoskeletal network by centrifugation. The S, I, and P fractions were then subjected to immunoprecipitation with the indicated antibodies and analyzed with streptavidin-peroxidase.

DNA constructs and ectopic expression with recombinant viruses

Human ICAM-3 complementary DNA was used as template to amplify the complete coding region of ICAM-3 by the polymerase chain reaction using specific oligonucleotides with additional sequences to create one *Hin*dIII and one *Eco*RI site at the 5′ and 3′ ends, respectively, of the amplification product. After digestion with *Hin*dIII and *Eco*RI, the DNA was cloned into the pEGFP-N1 vector (Clontech Laboratories, Palo Alto, CA) generating an in-frame fusion of green fluorescent protein (GFP) to the carboxyl terminus of ICAM-3. The fused ICAM-3/EGFP DNA was sequenced to rule out the possibility of amplification errors. The ICAM-3/EGFP DNA was excised from the vector by digestion with *Hin*dIII and *Stu*I and the DNA fragment was cloned into the pRB21 plasmid (kindly provided by Dr J. A. Melero, Instituto de Salud Carlos III, Madrid, Spain). The resulting construct was inserted into the defective vRB12 strain of vaccinia virus by homologous recombination. Recombinant viruses were selected by their ability to form lysis plaques. Viruses were then cloned, purified, and titered on CV1 cell monolayers. For infection with recombinant vaccinia virus, T cells were washed in infection medium (RPMI 1640 1% human serum albumin), resuspended at 1.0 × 10^6 cells/mL in infection medium, and infected at 10 plaque-forming units/cell at 37°C with occasional stirring. After 90 minutes, cells were washed extensively, resuspended in RPMI 1640/0.5% FCS and plated on coverslips coated with 20 μg/mL fibronectin.

Immunofluorescence analysis

Cells adhered to poly-L-lysine–coated coverslips were fixed in 4% (wt/vol) paraformaldehyde, rinsed, and treated with 10 mM glycine. Cells were washed, permeabilized or not with 0.2% Triton X-100, and incubated with 3% bovine serum albumin. Cells were sequentially incubated with the appropriate primary and secondary antibodies. For double-label immunofluorescence analysis, the procedure was repeated with the second primary and secondary antibodies. To visualize the distribution of cholesterol, T lymphoblasts were incubated with 5 μg/mL filipin for 10 minutes and, after extensive washing, cells were examined under UV light excitation.[33] Coverslips were mounted on slides and cells were photographed with a Zeiss Axioskop photomicroscope. Controls to assess the specificity of the labeling included incubations with control primary antibodies or omission of the primary antibodies.

Time-lapse fluorescence videomicroscopy

Coverslips were mounted on Attofluor open chambers (Molecular Probes) and placed on the microscope stage. Cells were maintained at 37°C in a 5% CO_2 atmosphere. Series of fluorescence and differential interference contrast frames were obtained simultaneously, using a Leica TCS-SP confocal laser scanning unit attached to a Leica DMIRBE inverted epifluorescence microscope, at 1-minute intervals immediately after addition of CD to the culture medium. Optical sectioning of cells was necessary to capture all the fluorescence signal. This was accomplished by acquiring series of 3 frames at 0.4-μm intervals through the cell. A projection of the fluorescence frames is presented with a single differential contrast image correspondent to the middle fluorescence frame to visualize the cell morphology.

Chemotaxis assay

Assays for lymphocyte chemotaxis were performed in polycarbonate membranes, of 6.5 mm diameter and 10 μm thickness, in 5-μm diameter pore size Transwell cell culture chambers (Costar, Corning, New York). Lymphocytes (100 μL at 7.5×10^5 cells/mL) suspended in RPMI 1640/0.5% human serum albumin were added to the upper chamber. Chemokines at the indicated concentrations (100 ng/mL for SDF-1α and 20 ng/mL for RANTES) in 600 μL RPMI 1640/0.5% human serum albumin were added to the lower chamber. Thereafter, the cells were allowed to migrate for 3 hours at 37°C in 5% CO_2 atmosphere. Then, the migrated cells were recovered from the lower part of the chemotaxis chamber and counted by flow cytometry.

Aggregation assay

Cells were washed twice in RPMI 1640 and resuspended to a final concentration of 1.0×10^6 cells/mL in RPMI 1640/10% FCS. Aliquots of 100 μL of the cell suspension were added to each well of flat-bottomed 96-well microtiter plates (Costar). Anti–ICAM-3 HP2/19 mAb at 1 μg/mL was added and the cells were allowed to settle at 37°C in 5% CO_2 atmosphere. Photomicrographs were taken at different times with a photo camera (Nikon) coupled to the microscope to follow the formation of cell aggregates.

Results

HA is selectively targeted to the uropod, a cholesterol-enriched structure, in T lymphoblasts

A human T lymphoblast pool consisting of approximately 40% of cells with a morphologic polarized phenotype and 60% of spherical cells was infected with influenza virus and the distribution of HA on the cell surface examined by immunofluorescence analysis in unpermeabilized cells. A polarized distribution of HA to a specific surface subdomain was observed in every cell in the culture, regardless of the morphology of the T cell. Figure 1 shows in a representative T lymphoblast with polarized shape that this subdomain corresponded to the uropod pole, at the trailing edge of the cell, as revealed by its colocalization with the uropod marker ICAM-3. In spherical blasts and Jurkat cells, HA was found

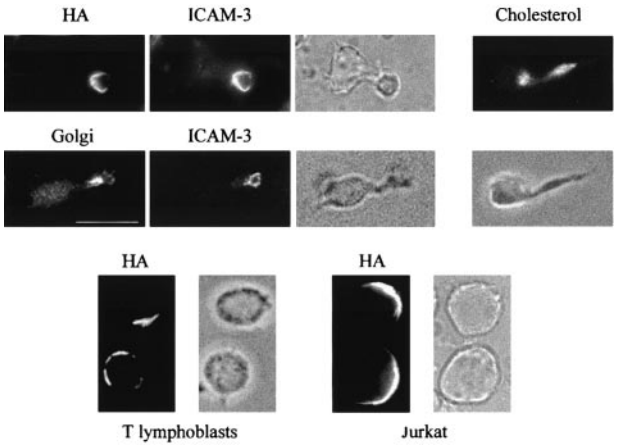

Figure 1. HA is selectively transported to the uropod in polarized T lymphoblasts. Human T lymphoblasts or Jurkat cells were infected with influenza virus for 4 hours at 37°C. Unpermeabilized T lymphoblasts were fixed and subjected to double labeling with mouse anti-HA mAb and rabbit anti–ICAM-3 antibodies. After permeabilization with 0.2% Triton X-100, T-cell blasts were analyzed with filipin to stain the cellular cholesterol, or double-labeled with anti-Golgi 58K and anti–ICAM-3 antibodies. Spherical blasts and Jurkat cells (bottom panels) were labeled with anti-HA antibodies in the absence of permeabilization step. To show cell morphology bright field images are depicted. Bar is 10 μm.

polarized to one hemisphere of the cell. Cholesterol, one of the major lipid components of rafts, predominantly distributed in the uropod structure as revealed with the cholesterol-binding drug filipin, which becomes fluorescent on UV light excitation. The uropod also contains the Golgi apparatus as evidenced by double staining with antibodies to the 58K Golgi marker and ICAM-3 (Figure 1).

HA incorporates into lipid rafts during biosynthetic transport to the T-cell surface

Internal lipid rafts have been proposed as being platforms for polarized apical delivery of proteins in epithelial MDCK cells.[22] HA and other proteins using this pathway become insoluble during biosynthetic transport as they are included in lipid rafts when they traverse the Golgi apparatus en route to the plasma membrane in epithelial cells.[21,23] Because a similar route of transport has not been described so far in T lymphocytes, it is not obvious which pathway is used for delivery of HA to the T-cell surface. The selective targeting of HA to a specific surface subdomain in T cells prompted us to investigate whether newly synthesized HA uses lipid rafts for biosynthetic transport in T cells. Jurkat cells were infected with influenza virus and cells were pulsed with (^{35}S)methionine/cysteine and chased for different times in the absence of radioactive precursors. At each time point, cells were lysed with 1% Triton X-100 and the S and I (raft) fractions were separated by centrifugation to equilibrium in sucrose density gradients.[21] Figure 2A shows that 10 minutes after biosynthesis, HA was already detected in the raft fraction and its presence in this fraction progressively increased after longer chase periods. To correlate the acquisition of insolubility of HA with its biosynthetic transport to the cell surface, metabolically labeled Jurkat cells were incubated with sulfo-NHS-biotin at the end of each of the chase periods to label surface proteins. Biotinylated molecules from the insoluble fractions were then immunoprecipitated with streptavidin-agarose and the immunoprecipitates subjected to SDS-PAGE and autoradiography to detect the arrival of newly synthesized HA to the cell surface. Figure 2B shows that there is a 20-minute lag between acquisition of insolubility (probably occurring in the Golgi), which was detected 10 minutes after biosynthesis (Figure 2A), and the arrival of HA at the cell surface (Figure 2B). Thus, recruitment into rafts precedes the arrival of HA to the cell surface suggesting, as in the case of

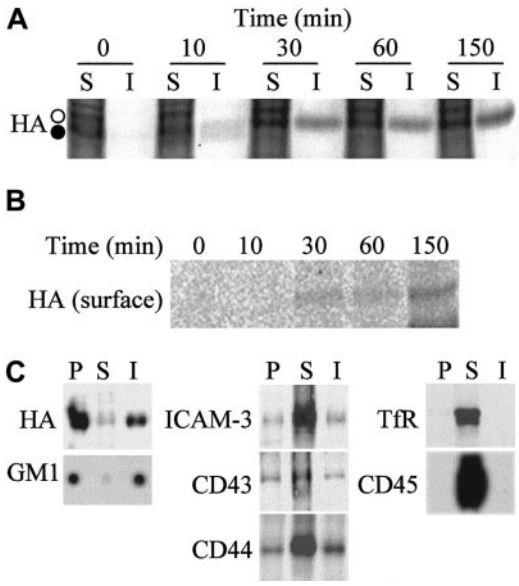

Figure 2. HA becomes incorporated into lipid rafts during biosynthetic transport to the plasma membrane in T cells. (A) After 3 hours of infection with influenza virus, Jurkat cells metabolically labeled with a 5-minute pulse of (^{35}S)methionine/cysteine were incubated for the indicated times in normal medium lacking radioactive precursors. Equivalent aliquots from the soluble (S) and the insoluble lipid raft (I) fractions were subjected to SDS-PAGE, and HA was detected by autoradiography. The position of the core-glycosylated and endoglycosidase H-resistant forms of HA are indicated by solid and empty circles, respectively. (B) Infected cells were metabolically labeled as in panel A. At the end of each chase period, surface proteins were biotinylated, and the lipid raft fraction was immunoprecipitated with streptavidin-agarose. The arrival of radiolabeled HA at the cell surface was monitored by autoradiography of the immunoprecipitates. HA was easily identified due to the profound shut-off of host protein synthesis induced by influenza virus infection. (C) T lymphoblasts were infected for 4 hours, and then surface proteins were biotinylated. After centrifugation to equilibrium, the soluble (S) and floating raft (I) fractions, and the cytoskeleton-associated rafts (P) were subjected to immunoprecipitation with antibodies specific to the indicated proteins and immunoblotted with streptavidin-peroxidase or analyzed with cholera toxin B subunit coupled to peroxidase to detect GM1.

polarized MDCK cells, a role for rafts in the biosynthetic transport of HA.

The accumulation of HA in the uropod region led us to analyze the residence of surface HA and endogenous surface uropod markers in lipid rafts at steady state. At least a fraction of uropod surface markers is associated with cytoskeletal elements.[3] To study the association of uropod proteins with surface rafts, in addition to the floating lipid raft fraction (I), the rafts associated with cytoskeleton (P) were also analyzed. Surface proteins of T lymphoblasts were labeled with sulfo-NHS-biotin, and then the cells were lysed with 0.2% Triton X-100 in the cold. The extract was centrifuged to equilibrium in a sucrose density gradient, equivalent aliquots from the S, I, and P fractions were immunoprecipitated with antibodies to ICAM-3, CD43, CD44, or HA, and the immunoprecipitates were analyzed with streptavidin-peroxidase to detect surface proteins. Figure 2C shows that, in addition to surface HA, significant levels of 3 endogenous uropod proteins, ICAM-3, CD43, and CD44, were detected in the fractions containing surface rafts. As controls, the glycolipid GM1 was found exclusively confined to rafts, whereas CD45 and the transferrin receptor, which are evenly distributed on the cell surface, were excluded.

Lipid raft integrity is necessary for the induction and maintenance of the T- lymphoblast shape asymmetry

The capacity of CD to sequester cholesterol from cellular membranes has been exploited to alter the integrity of lymphocyte lipid rafts.[29-31] The lipid raft-mediated apical pathway of transport of HA in epithelial cells has been shown to be dependent on normal cholesterol levels because the removal of cholesterol with CD disrupts the association of HA with rafts and results in its reduced apical transport and partial missorting to the basolateral surface.[24] Using CD we first investigated the requirement of lipid raft integrity in the generation of a polarized morphology in T lymphoblasts stimulated by either ICAM-3 cross-linking or incubation with the SDF-1α chemokine, 2 treatments known to increase the number of polarized cells.[9] Figure 3 shows that after 1 hour of treatment the percentage of uropod-bearing T-cell blasts increased from approximately 40% in untreated cells (Figure 3A) to about 80% in ICAM-3 cross-linked cells (Figure 3C) or 70% in cells treated with SDF-1α (Figure 3E). This de novo–induced polarization was completely abolished in cells whose cholesterol levels were decreased by pretreatment with 8 mM CD (Figure 3D,F). Formation of uropod structures was restored when cells pretreated with CD and subjected to ICAM-3 cross-linking were incubated in normal medium containing 20% FCS for 24 hours (Figure 3G), thus indicating that cells remain viable after CD treatment and that the effect of CD on the induction of the polarized phenotype was reversible. It is of special note that cholesterol depletion not only affects the de novo polarization process but also greatly reduces the number of pre-existing polarized cells in the culture (Figure 3B). Panel H in Figure 3 shows the filipin staining pattern obtained in control and CD-treated T lymphoblasts to illustrate the efficiency of CD in the extraction of cholesterol. Panel I in Figure 3 shows a quantitative analysis of the percentage of uropod-bearing cells under the different treatments used.

To analyze whether the effect of CD on the T-cell morphology was paralleled by alterations of the cytoskeleton, we compared the arrangement of the microtubule and actin cytoskeleton before and after the treatment with CD using immunofluorescence analysis with antibodies specific to α- and γ-tubulin or with phalloidin,

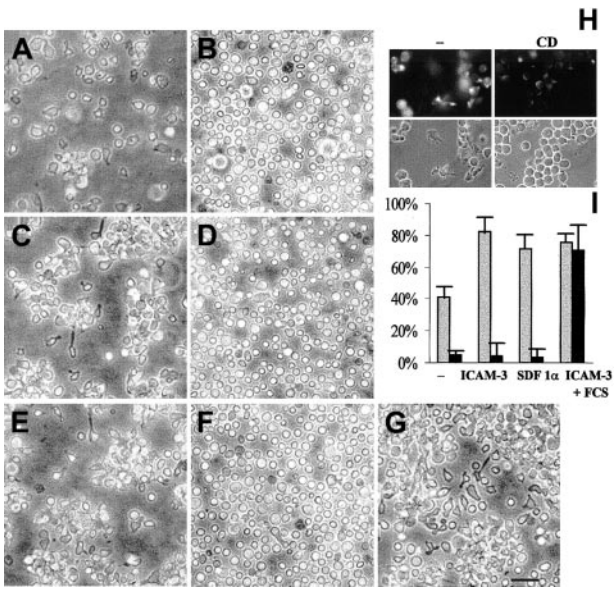

Figure 3. Cholesterol sequestration prevents the induction of uropod structures in T lymphoblasts. Control (A,B) or T lymphoblasts stimulated with 100 ng/mL SDF-α (C,D) or 1 μg/mL anti–ICAM-3 HP2/19 mAb (E-G) were treated (B,D,F,G) or not (A,C,E) with 8 mM CD in RPMI medium. After CD treatment, part of the cell culture stimulated with anti–ICAM-3 HP2/19 mAb was washed and incubated in RPMI medium supplemented with 20% FCS in the absence of CD (G). Bar is 20 μm. Panel H shows the cholesterol levels, as detected by staining with filipin, in control (−) or in T lymphoblasts treated with CD. Bright field images are depicted to show the cell field. The presence of uropod in approximately 500 cells was analyzed in 3 independent replicates. The results obtained in untreated (gray bars) and CD-treated (black bars) cells are represented as percentage of uropod-bearing cells present in the culture (I). The mean ± SD is shown.

respectively. Figure 4 shows that in parallel with the change in the lymphoblast morphology, the microtubule and actin cytoskeleton networks rearranged in CD-treated cells but they did not disassemble and the microtubule-organizing center remained intact.

Unclustering of ICAM-3 precedes the disassembly of the uropod induced by disruption of lipid rafts

To analyze simultaneously the kinetics of uropod disassembly and ICAM-3 redistribution in T lymphoblasts after cholesterol depletion, we used recombinant vaccinia virus to express a chimera consisting of ICAM-3 fused at its carboxyl terminus with GFP (ICAM-3/GFP). The distribution of ICAM-3/GFP and the uropod architecture were monitored by live 3-dimensional fluorescence microscopy. The clustering of surface ICAM-3/GFP at the uropod tip in untreated cells was similar to that of the endogenous ICAM-3 molecule. Figure 5 shows that surface ICAM-3/GFP remained mostly clustered at the uropod tip 15 minutes after CD addition. After an additional 15 minutes in the presence of CD, a fraction of ICAM-3/GFP adopted a less clustered distribution despite the uropod structure still being evident. Finally, after 45 minutes of treatment, the uropod was completely retracted and ICAM-3/GFP achieved an even distribution on the cell surface. These effects were not observed in the absence of CD treatment (Figure 5). The intense labeling in the Golgi area, due to the massive synthesis of ICAM-3/GFP directed by the virus, was observed regardless of whether the cells were treated with CD or not. These results indicate that raft disruption causes first the unclustering of ICAM-3 in the uropod and then its redistribution to other surface regions, and that these processes precede the disappearance of the uropod structure.

Intact lipid rafts are required for aggregation and migration of T lymphoblasts

In response to certain stimuli, T lymphoblasts initiate locomotion on the substratum, acquire a polarized morphology, and establish early cell-cell interactions through their uropods, forming motile small aggregates.[14] Before 1 hour of treatment, exposed uropods from those motile aggregates contact with others generating large

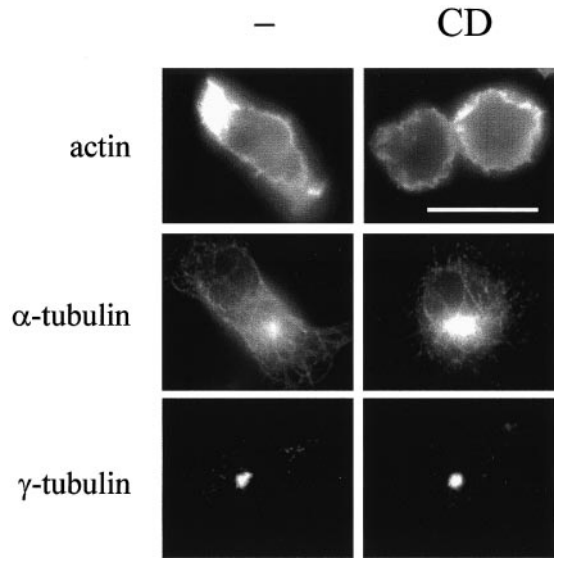

Figure 4. Cholesterol sequestration induces the rearrangement of the cytoskeleton but not its disassembly in polarized T lymphoblasts. Control or T lymphoblasts treated for 30 minutes with 8 mM CD were subjected to immunofluorescence analysis with fluorescent phalloidin to detect F-actin, or with antibodies to α- or γ-tubulin to stain the microtubule network or the microtubule-organizing center, respectively. Bar is 12 μm.

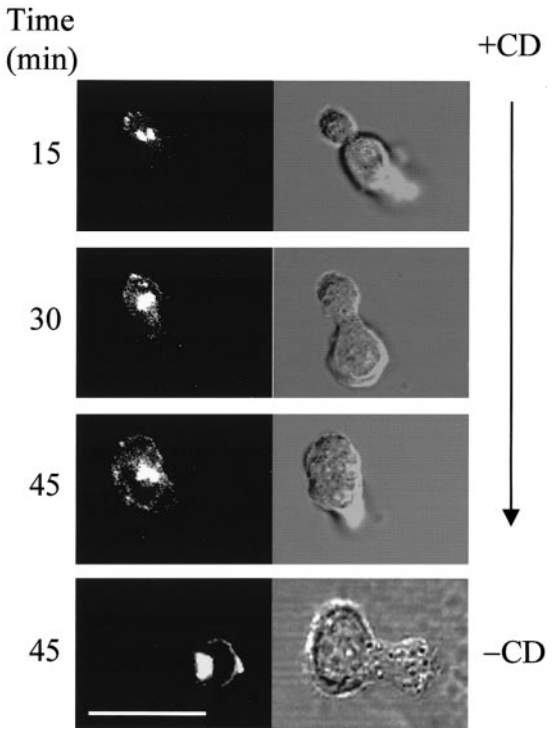

Figure 5. Dynamics of ICAM-3 redistribution in CD-treated T lymphoblasts. T cells infected with recombinant vaccinia virus expressing ICAM-3/GFP for 2 hours at 37°C were treated or not with CD and analyzed by live 3-dimensional fluorescence microscopy at the indicated times after the addition of CD. Bar is 12 μm.

cellular aggregates.[14] To analyze the requirement for raft integrity in this process, T lymphoblasts were treated or not with CD and, after removal of the drug, cell aggregation was induced with anti–ICAM-3 HP2/19 mAb for 30 minutes. Controls incubated in the absence of mAb or with the nonpolarizing anti–ICAM-3 TP1/24 mAb, which does not promote cell aggregates, were analyzed at the same time in parallel. Figure 6A shows that disruption of lipid rafts by CD treatment severely interferes with lymphocyte recruitment both in control cells and in cells stimulated with the anti–ICAM-3 HP2/19 mAb. The inhibition of aggregation caused by CD treatment was reversible and the cell viability was unaffected because after 2 hours of incubation in the presence of 10% FCS, CD-treated cells recovered their aggregation properties.

Lymphocyte switching from a spherical to a uropod-containing morphology in response to chemotactic or proinflammatory chemokines correlates with increased migratory capacity.[9] To determine whether raft disruption interferes with lymphocyte chemotaxis, migration assays using the SDF-1α and RANTES chemokines were performed in the presence or absence of CD in cells incubated in Transwell cell culture chambers of 5-μm pore diameter. Cells that traversed the chamber were counted after 2 hours of chemokine stimulation, the time of optimal response. As shown in Figure 6B, T-lymphoblast chemotaxis was dramatically reduced by cholesterol sequestration in both nonstimulated and RANTES-stimulated cells. When cells were activated with SDF-1α a stronger chemotactic stimulus than that of RANTES, migration of CD-treated cells significantly diminished to approximately 30% of that of untreated blasts.

Discussion

The question of how segregation of surface molecules occurs in a polarized cell has been one of the main foci of modern cell

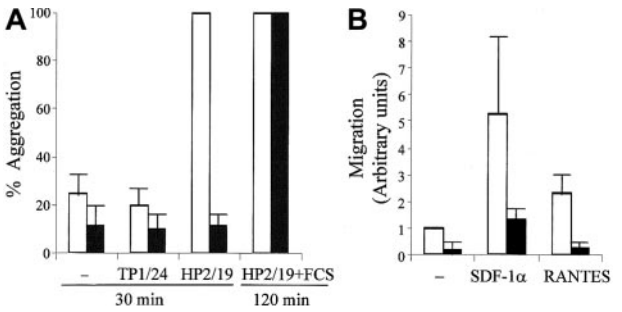

Figure 6. Lipid raft integrity is necessary for uropod-mediated adhesion and T-cell chemotaxis. (A) T lymphoblasts were treated or not with CD and, after extensive washing to remove the drug, cell aggregation was induced with anti–ICAM-3 HP2/19 mAb for 30 minutes. Cultures incubated in the absence of mAb or with the control anti–ICAM-3 TP1/24 mAb were analyzed in parallel. A control of anti–ICAM-3 HP2/19 mAb-stimulated cells incubated for 2 hours in the presence of 10% FCS after CD treatment shows that the effect of CD was reversible. The numbers of cell aggregates were quantified in the untreated (white bars) and CD-treated cultures (black bars) and represented as the percentage of aggregates relative to those in the untreated cells stimulated with anti–ICAM-3 HP2/19 mAb. (B) Cells treated or not with CD were induced to migrate toward SDF-1α or RANTES for 2 hours. The numbers of migrated cells in the untreated (white bars) and CD-treated cultures (black bars) were determined and expressed in arbitrary units. The mean ± SD of 4 independent replicates using T lymphoblasts prepared from peripheral blood lymphocytes obtained from different donors is shown in panels A and B.

biology.[34,35] In epithelial cells, targeting to the apical surface for at least some membrane proteins appears to be mediated by their partitioning into lipid rafts during biosynthetic transport.[21,23] Interestingly, even cell types that lack distinguishable apical and basolateral subdomains, such as fibroblasts, share apical and basolateral cognate routes to the plasma membrane with polarized epithelia.[36,37] This suggests that, although protein sorting machinery might differ between cell types, membrane traffic mechanisms are basically conserved in most cell types. In T cells, lipid rafts have been implicated in the recruitment of molecules involved in signaling pathways during activation.[29-31] Despite the remarkable polarization of the T-cell surface during the processes of antigen recognition, chemotaxis, transmigration, and interaction with other leukocytes,[3,8] the involvement of lipid rafts in the selective targeting of surface molecules to different poles and their role in the establishment of T- cell polarity has not been investigated. In this study we have used the prototypical HA marker as a tool to explore the existence of a route in T cells reminiscent of the raft-mediated apical pathway of epithelial cells. We have observed that HA is targeted to a specific surface subdomain, regardless of the polarized or unpolarized morphology of the T lymphocyte. In T cells with polarized shape, this subdomain localized to the uropod pole. Similar to epithelial cells, HA became partially integrated into insoluble lipid rafts during biosynthetic transport to the plasma membrane in T lymphocytes, and remained partially insoluble once at its destination. Consistent with the existence of a raft-mediated biosynthetic pathway of transport to the plasma membrane, the Golgi apparatus and cholesterol, one of the major lipid components of rafts, distributed in the uropod. In addition to HA, the surface ICAM-3, CD44, and CD43 uropod markers were detected in the insoluble raft fraction, whereas the tyrosine phosphatase CD45 and the transferrin receptor, whose distribution is not polarized, were completely excluded from lipid rafts. Thus, T lymphocytes appear to have a lipid raft–mediated pathway functional for transporting cargo to the uropod surface, which, similar to the apical surface of polarized cells, also contains lipid rafts. The MAL proteolipid has been recently identified as an essential component of the integral protein machinery for the raft-mediated apical pathway in epithelial MDCK cells.[25-28] The fact that, despite the restricted range of transcription of the *MAL* gene, MAL is expressed not only in polarized epithelia but also in T lymphocytes[38] and is present in lipid rafts in T cells[39,40] is consistent with a possible role for MAL in protein transport to the T-cell uropod.

Intact lipid rafts are required for a variety of processes including apical transport of certain molecules,[21,23] T-cell activation,[29-31] and front-rear polarity in breast adenocarcinoma MCF-7 cells.[41] The identification of a raft-mediated pathway of transport to the uropod led us to examine the effect of the disruption of lipid rafts on the morphology of T lymphoblasts. Sequestration of cholesterol with CD produced a complete block of the de novo formation of uropod structures induced by either SDF-1α treatment or ICAM-3 cross-linking but did not cause disassembly of the cytoskeleton. The fact that we observe raft polarization even in T cells lacking uropods indicates that raft clustering is necessary but not sufficient for uropod formation. The establishment of a polarized morphology probably requires, in addition to raft clustering, a rearrangement of the cytoskeleton to maintain the polarized cell architecture and to stabilize the clustered rafts in the uropod. The effect of sequestration on the de novo formation of uropod structures induced by either SDF-1α treatment or ICAM-3 cross-linking paralleled with a dramatic impairment in the capacity of the cells to interact with other T cells, a process known to be mediated by adhesion receptors, such as ICAM-3, localized to the uropod. It is of special note that the treatment with CD did not affect the levels of ICAM-3 on the cell surface (not shown), indicating that the presence of ICAM-3 in the uropod is necessary for T-cell adhesion.

The T-cell uropods appear to emerge as protrusions disposed "apically" with respect to the flattened cell body and perpendicularly to the endothelium monolayer, to recruit naive cells from the bloodstream.[7,32] In this way, polarized T cells increase their volume and become exposed to a hemodynamic stress that has even been proposed as being an additional modulating signal.[42] As is the case for epithelial cells, whose apical subdomain is enriched in lipid rafts components[43] and faces the harsh extracellular environment, it is plausible that polarized T cells use lipid rafts not only for selective sorting of receptors to the uropod but also to protect this subdomain from the harsh environment of the circulatory flow. Consistent with our data showing accumulation of raft-associated proteins in the uropod tip, recent evidence indicates preferential budding of human immunodeficiency virus type 1 from lipid rafts located in the uropod.[44] This suggests that the uropod is a versatile surface specialization that can be used for many different processes. We and others have reported heterogeneity in the lipid rafts present on the T-cell surface.[45-47] It is likely that the rafts that concentrate T-cell receptor signaling machinery at steady state are different from those present in the uropod tip. In fact, the rafts containing the T-cell receptor appear to be more labile to detergent extraction than those found in the uropod.[48] Because T-cell costimulation induces raft aggregation at the contact site,[49] an interesting possibility is that the rafts in the uropod redistribute to the contact site on costimulation to sustain the T-cell activation process. The fact that T cells lack discernible structures similar to tight junctions, which prevent intermixing of the components of the apical and basolateral subdomains by lateral diffusion in polarized epithelia,[17] suggests the existence of another type of "fence" in T cells probably related to that proposed to exist in neurons and other cell types without tight junctions.[50]

Because of the highly specialized functions of T lymphocytes, the movement of a T cell implies not only rolling, tethering, or transmigration but also sticking and recruitment of other bystander lymphoid cells. The uropod is a specialized surface subdomain involved in these specialized tasks, similar to the apical surface that is in charge of most of the specialized functions (filtration,

absorption, and secretion) of epithelial cells. For these purposes, the uropod requires a specific set of molecules and the existence of mechanisms to maintain its unique structure and composition. Our results show that (1) there is biosynthetic pathway of transport to the uropod tip mediated by lipid rafts, (2) endogenous uropod markers are detected in lipid rafts, (3) the clustering of ICAM-3 at the uropod is rapidly lost when lipid raft integrity is disrupted, (4) intact lipid rafts are required for the de novo formation and maintenance of the uropod structures, and (5) lipid raft integrity is necessary for T-cell processes that require a polarized phenotype, such as intercellular aggregation and migration.

Acknowledgment

We thank Sergio Gómez for expert technical help.

References

1. Rodriguez-Boulan E, Powell SK. Polarity of epithelial and neuronal cells. Ann Rev Cell Biol. 1992;8:395-427.
2. Bretscher MS. Getting membrane flow and the cytoskeleton to cooperate in moving cells. Cell. 1996;87:601-606.
3. Sánchez-Madrid F, del Pozo MA. Leukocyte polarization in cell migration and immune interactions. EMBO J. 1999;18:501-511.
4. Lowin-Kropf B, Shapiro VS, Weiss A. Cytoskeletal polarization of T cells is regulated by an immunoreceptor tyrosine-based activation motif-dependent mechanism. J Cell Biol. 1998;140:861-871.
5. Mitchison TJ, Cramer LP. Actin-based cell motility and cell locomotion. Cell. 1996;84:371-379.
6. Bretscher MS, Aguado-Velasco C. Membrane traffic during cell locomotion. Curr Opin Cell Biol. 1998;10:537-541.
7. del Pozo MA, Nieto M, Serrador JM, et al. The two poles of the lymphocyte: specialized cell compartments for migration and recruitment. Cell Adhes Commun. 1998;6:125-133.
8. Negulescu PA, Kasieva TB, Khan A, Kerschbaum HH, Cahalan MD. Polarity of T cell shape, motility, and sensitivity to antigen. Immunity. 1996;4:421-430.
9. Nieto M, Frade JMR, Sancho D, Mellado M, Martinez-A C, Sánchez-Madrid F. Polarization of chemokine receptors to the leading edge during lymphocyte chemotaxis. J Exp Med. 1997;186:153-158.
10. Campanero MR, Sánchez-Mateo P, del Pozo MA, Sánchez-Madrid F. ICAM-3 regulates lymphocyte morphology and integrin mediated T-cell interaction with endothelial cell and extracellular matrix ligands. J Cell Biol. 1994;127:867-878.
11. del Pozo MA, Sanchez-Mateos P, Nieto M, Sánchez-Madrid F. Chemokines regulate cellular polarization and adhesion receptor redistribution during lymphocyte interaction with endothelium and extracellular matrix. Involvement of cAMP signaling pathway. J Cell Biol. 1995;131:495-508.
12. del Pozo MA, Sánchez-Mateos P, Sánchez-Madrid F. Cellular polarization induced by chemokines: a mechanism for leukocyte recruitment. Immunol Today. 1996;17:127-130.
13. Hedrick JA, Zlotnik A. Chemokines and lymphocyte biology. Curr Opin Immunol. 1996;8:343-347.
14. Serrador JM, Nieto M, Alonso-Lebrero JL, et al. CD43 interacts with moesin and ezrin and regulates its distribution to the uropods of T lymphocytes at the cell-cell contacts. Blood. 1998;91:4632-4644.
15. Borset M, Hjertner O, Yaccoby S, Epstein J, Sanderson RD. Syndecan-1 is targeted to the uropods of polarized myeloma cells where it promotes adhesion and sequesters heparin-binding proteins. Blood. 2000;96:2528-2536.
16. Parlato S, Giammarioli AM, Logozzi M, et al. CD95 (APO/Fas) linkage to the actin cytoskeleton through ezrin in human T lymphocytes: a novel regulatory mechanism of the CD95 apoptotic pathway. EMBO J. 2000;19:5123-5134.
17. Matter K, Mellman I. Mechanisms of cell polarity: sorting and transport in epithelial cells. Curr Opin Cell Biol. 1994;6:545-554.
18. Foletti DL, Prekeris R, Scheller RH. Generation and maintenance of neuronal polarity: mechanisms of transport and targeting. Neuron. 1999;23:641-644.
19. Simons K, Ikonen E. Functional rafts in cell membranes. Nature. 1997;387:569-572.
20. Brown DA, London E. Structure and function of sphingolipid- and cholesterol-rich membrane rafts. J Biol Chem. 2000;275:17221-17224.
21. Brown DA, Rose JK. Sorting of GPI-anchored proteins to glycolipid-enriched membrane subdomains during transport to the apical cell surface. Cell. 1992;68:533-534.
22. Simons K, Wandinger-Ness A. Polarized sorting in epithelia. Cell. 1990;62:207-210.
23. Skibbens JE, Roth MJ, Matlin KS. Differential extractability of influenza virus hemagglutinin during intracellular transport in polarized epithelial cells and nonpolar fibroblasts. J Cell Biol. 1989;108:821-832.
24. Keller P, Simons K. Cholesterol is required for surface transport in influenza virus hemagglutinin. J Cell Biol. 1998;140:1357-1367.
25. Puertollano R, Martín-Belmonte F, Millán J, et al. The MAL proteolipid is necessary for normal apical transport and accurate sorting of the influenza virus hemagglutinin in Madin-Darby canine kidney cells. J Cell Biol. 1999;145:141-145.
26. Cheong KH, Zacchetti D, Schneeberger EE, Simons K. VIP17/MAL, a lipid raft-associated protein, is involved in apical transport in MDCK cells. Proc Natl Acad Sci U S A. 1999;96:6241-6248.
27. Puertollano R, Alonso MA. MAL, an integral element of the apical sorting machinery, is an itinerant protein that cycles between the trans-Golgi network and the plasma membrane. Mol Biol Cell. 1999;10:3435-3447.
28. Martín-Belmonte F, Puertollano R, Millán J, Alonso MA. The MAL proteolipid is necessary for the overall apical delivery of membrane proteins in the polarized epithelial Madin-Darby canine kidney and Fischer rat thyroid cell lines. Mol Biol Cell. 2000;11:2033-2045.
29. Xavier R, Brennan T, Li Q, McCormack C, Seed B. Membrane compartmentation is required for efficient T cell activation. Immunity. 1998;8:723-732.
30. Montixi C, Langlet C, Bernard AM, et al. Engagement of T cell receptor triggers its recruitment to low density detergent insoluble membrane domains. EMBO J. 1998;17:5334-5348.
31. Moran M, Miceli MC. Engagement of GPI-linked CD48 contributes to TCR signals and cytoskeletal reorganization: a role for lipid rafts in T cell activation. Immunity. 1998;9:787-796.
32. del Pozo MA, Cabañas C, Montoya MC, Ager A, Sánchez-Mateos P, Sánchez-Madrid F. ICAMs redistributed by chemokines to cellular uropods as a mechanism for recruitment of T lymphocytes. J Cell Biol. 1997;137:493-508.
33. Blanchette-Mackie EJ, Dwyer NK, Amende LM, et al. Type-C Niemann-Pick disease: low density lipoprotein uptake is associated with premature cholesterol accumulation in the Golgi complex and excessive cholesterol storage in lysosomes. Proc Natl Acad Sci U S A. 1988;85:8022-8026.
34. Drubin DG, Nelson WJ. Origins of cell polarity. Cell. 1996;84:335-344.
35. Eaton S, Simons K. Apical, basal, and lateral cues for epithelial polarization. Cell. 1995;82:5-6.
36. Yoshimori T, Keller P, Roth MG, Simons K. Different biosynthetic transport routes to the plasma membrane in BHK and CHO cells. J Cell Biol. 1996;133:247-256.
37. Müsch A, Xu H, Shields D, Rodriguez-Boulan E. Transport of vesicular stomatitis virus G protein to the cell surface is signal mediated in polarized and nonpolarized cells. J Cell Biol. 1996;133:543-558.
38. Alonso MA, Weissman SM. cDNA cloning and sequence of MAL, a hydrophobic protein associated with human T-cell differentiation. Proc Natl Acad Sci U S A. 1987;84:1997-2001.
39. Millán J, Puertollano R, Fan L, Rancaño C, Alonso MA. The MAL proteolipid is a component of the detergent-insoluble membrane subdomains of human T lymphocytes. Biochem J. 1997;321:247-252.
40. Millán J, Alonso MA. MAL, a novel integral membrane protein of human T lymphocytes, associates with glycosylphosphatidylinositol-anchored proteins and Src-like tyrosine kinases. Eur J Immunol. 1998;28:3675-3684.
41. Mañes S, Mira E, Gómez-Mouton C, et al. Membrane raft microdomains mediate front-rear polarity in migrating cells. EMBO J. 1999;18:6211-6220.
42. Von Andrian UH. A massage for the journey: keeping leukocytes soft and silent. Proc Natl Acad Sci U S A. 1997;94:4825-4827.
43. Simons K, van Meer G. Lipid sorting in epithelial cells. Biochemistry. 1988;27:6197-6202.
44. Nguyen DH, Hildreth JEK. Evidence for budding of human immunodeficiency virus type 1 selectively from glycolipid-enriched membrane lipid rafts. J Virol. 2000;74:3624-3272.
45. Cerny J, Stockinger H, Horejsi V. Noncovalent associations of T lymphocyte surface proteins. Eur J Immunol. 1996;26:2335-2343.
46. Millán J, Cerny J, Horejsi V, Alonso MA. CD4 segregates into specific detergent-resistant T-cell membrane microdomains. Tissue Antigens. 1999;53:33-40.
47. Millán J, Quaidi M, Alonso MA. Segregation of costimulatory components into specific T-cell surface lipid rafts. Eur J Immunol. 2001;31:467-473.
48. Janes PW, Ley SC, Magee AI. Aggregation of lipid rafts accompanies signaling via the T cell antigen receptor. J Cell Biol. 1999;147:447-461.
49. Viola A, Schroeder S, Sakakibara Y, Lanzavecchia A. T lymphocyte costimulation mediated by reorganization of membrane microdomains. Science. 1999;283:680-682.
50. Winckler B, Mellman I. Neuronal polarity: controlling the sorting and diffusion of membrane components. Neuron. 1999;23:637-640.

2002 99: 978-984
doi:10.1182/blood.V99.3.978

Lipid rafts mediate biosynthetic transport to the T lymphocyte uropod subdomain and are necessary for uropod integrity and function

Jaime Millán, Mari?a C. Montoya, David Sancho, Francisco Sánchez-Madrid and Miguel A. Alonso

Blood (print ISSN 0006-4971, online ISSN 1528-0020), is published weekly by the American Society of Hematology, 2021 L St, NW, Suite 900, Washington DC 20036.